

# MIXED CONVECTION IN A FULL SCALE AIRCRAFT CABIN MOCK-UP

**J. Bosbach, M. Kühn, M. Rütten, C. Wagner**

**German Aerospace Center (DLR), Institute of Aerodynamics and Flow Technology,  
Bunsenstr. 10, 37073 Göttingen, Germany**

**Keywords:** *mixed convection, indoor air flow, large scale PIV*

## Abstract

*For the study of mixed convective airflows, a full scale double aisle aircraft cabin mock-up has been built at the German Aerospace Center in Göttingen. It is designed as a testing configuration with realistic boundary conditions for commercial Computational Fluid Dynamics (CFD)-codes as well as the DLR in house code THETA. The aim is the reliable prediction of cabin air-flow by means of CFD under consideration of computational time. Special attention will be given to the proper prediction of the separation lines as well as the resulting temperature distribution, making necessary validation of the used turbulence and radiation models. In order to provide a comprehensive validation data base the flow in the mock-up was studied with Particle Image Velocimetry (PIV), infrared thermography, and field temperature measurements. The influence of buoyancy effects and the interaction of the incoming air jets on the flow field have been studied independently by switching from isothermal to cooling conditions and by a systematical variation of the relative volume flow of the air inlets.*

## 1 Introduction

During the development of modern aircrafts passenger comfort plays an increasing role. The rising demand of the airlines for individual cabin designs leads to faster development cycles. In order to ensure the thermal comfort, computer based methods come into play, which are demanding with respect to numerical cost and are thus developed mainly by large research

facilities and software suppliers. The quality of these simulation tools relies on the availability of corresponding test data.

For thermal comfort air distribution is one of the most important factors. Since the flow in occupied ventilated spaces is characterized by superposition of natural convection due to the heat load of the occupants and forced convection due to the ventilation system, validation data has to be acquired at full scale. As a consequence detailed measurements of mixed convection at full model scale are necessary. Since the cabin air flow can be easily disturbed, non-intrusive optical field measurement methods have to be used preferably. Particle Image Velocimetry (PIV), Particle Tracking Velocimetry (PTV), and Particle Streak Velocimetry (PSV) have been applied to measure the air flow in aircraft cabins recently by different researchers:

Velocity and turbulence intensity profiles were measured by Mo et al. in a narrow body (737) aircraft cabin section on FOVs of 0.6 x 0.6 m<sup>2</sup> by illuminating thermoplastic shell particles with a pulsed Xenon flash lamp [1].

Müller et al. used two component PTV in order to measure velocity fields of the flow in an A330/A340 mock-up section [2]. Helium filled soap bubbles (HFSBs) with diameters between 3 and 7 mm were illuminated by spot lamps in order to measure the fluid velocity. With a light sheet thickness of 0.7 m a FOV of 1x1.5 m<sup>2</sup> was measured instantaneously with 100-200 Bubbles per image.

By increasing the efficiency of the HFSB generator with an advanced bubble generation nozzle, Müller et al. were able to perform PIV measurements of airflow in a preliminary A3xx

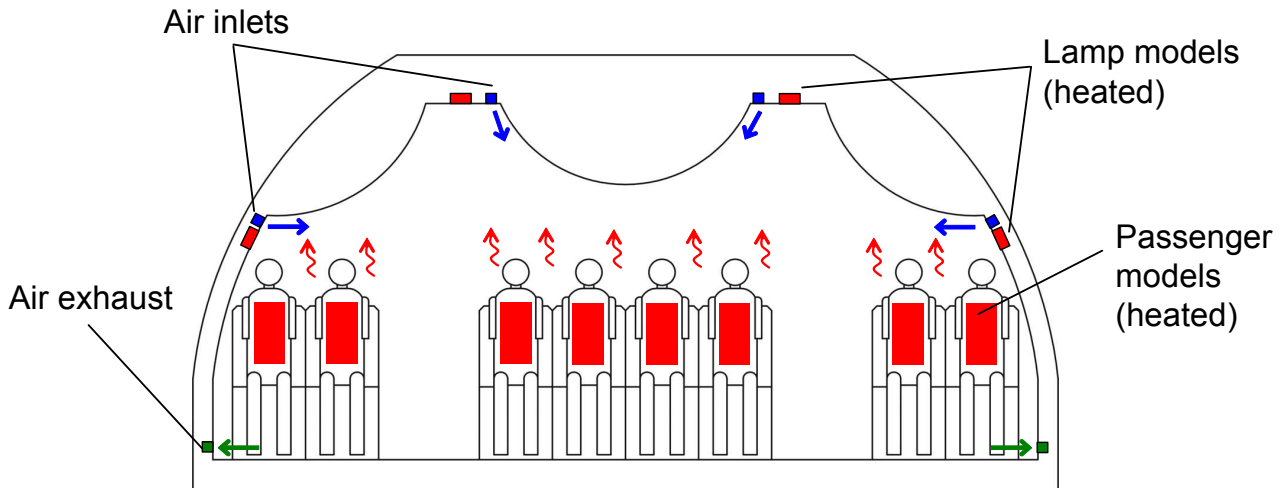


**Fig. 1.** Cross section of the generic A380 aircraft cabin model of the German Aerospace Center in Göttingen.

upper deck cabin section [3]. The light sheet thickness was set to less than 150 mm and the FOV amounted to about 2.35 m<sup>2</sup> per camera. Several halogen lamps were used in parallel for illumination.

Volumetric three component PSV has been performed to measure the air flow in a full scale Boeing 767 mock-up with five seat rows by Sun et al. and Zhang et al. [4][5]. A measurement volume of 1.8 x 4 x 2 m<sup>3</sup> was illuminated by 36 spot lights with an overall power of 4.32 kW. Since the particle density was as low as 120/m<sup>3</sup>, corresponding to 1800 particles in the whole measurement volume, instantaneous data could be obtained only at a very low information density. This can be a serious drawback if instationary phenomena as they usually occur in mixed convection or turbulent cabin flow are subject to investigation.

Image correlation techniques, like PIV, usually provide a better signal to noise ratio as compared to PSV or PTV and the ability to measure instantaneous velocity data with high spatial resolution [6]. Therefore for measurement of mixed convection in our aircraft cabin mock-up PIV has been performed at full scale by combination of HFSSBs as tracer particles with high power quality switched solid state lasers as light sources [7]. As a result velocity and velocity fluctuation fields at high spatial resolution have been measured in many different scenarios. The results serve as a data base for validation of the DLR in house CFD code THETA

(Turbulent Heat release Extension of the TAU-Code).

## 2 Generic A380 Aircraft Cabin Mock-Up

In order to provide a realistic test configuration with well defined boundary conditions for CFD validation a full scale double aisle aircraft cabin mock-up section has been built at the German Aerospace Center Göttingen.

### 2.1 General Set Up

The aircraft cabin mock-up was designed to be a generic replica of a section of the A380 upper deck. It has a width of 5.1 m, a length of 6 m, and a height of up to 2.2 m, its dimensions being slightly reduced as compared to the original. The interior of the cabin features five seat rows with two seats at both sides and four in the middle, separated by two aisles, see Fig. 1. Each of the 40 seats is occupied by a passenger dummy. Above the seats the ceiling is covered by generic overhead bin contours. The dummies are heated by two internal bulbs, one with a power of 15 W in the throat and one with a power of 40 W in the breast. This results in a heat load of 55 W per dummy and thus reflects the thermal load of the passengers in the real cabin. Further, the heat load due to light bands is realized by four electrical heating panels with a width of 100 mm each, supplying 1.8 kW of heat in total. All heating devices are operated in

constant heat flux mode. The 24 air inlets have a length of 920 mm and a width of 18 mm and are placed in four lines along the ceiling. The angle of the incoming air jets can be changed slightly. After circulation in the mockup, the air leaves through 12 air outlets with a width of 50 mm at the cabin floor. Flaps and measuring orifices (18 in total) control the flow rates of incoming and outgoing air. Optical access to the mock-up for flow visualization and PIV is provided by viewports at the front and the back face.

## 2.2 Parameters and Boundary Conditions

For the measurements described in the following, the air was supplied through the inlets at the ceiling and the lateral air inlets, see Fig. 1. All inlets were oriented parallel to the corresponding contour faces. The air exchange rate was set to 27 m<sup>3</sup>/h per passenger, corresponding to 23/h for the whole cabin. Having kept these values fixed, the relative mass flow between the air inlets has been changed systematically in order to investigate the influence on the overall flow pattern. The relative mass flow between the ceiling and the lateral air inlets has been varied in steps of 33 %, 50 % and 67 % relative mass flow, which corresponds to nominal inlet velocities of 0.65 m/s, 0.76 m/s, and 1.02 m/s, respectively.

All scenarios have been investigated under

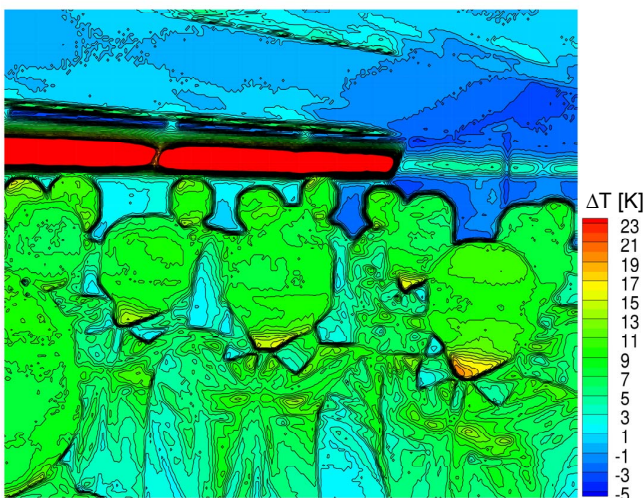


**Fig. 2.** Surface temperatures in the cabin mock-up as measured by infrared thermography for equally distributed volume flow. Temperatures are given as difference to the average cabin temperature.

isothermal conditions, where all heat sources were switched off, and under cooling conditions with the passenger dummies and the light band models switched on, i.e. with a heating power of 4 kW in total. By switching from the isothermal to the cooling case we were able to study the influence of buoyancy effects on the flow. Under cooling conditions, where the incoming air jets enter a warm cabin, the temperature difference between the cabin air and the incoming air amounted to  $6.35 \pm 0.35$  K.

The resulting surface temperatures of the passenger dummies and the light band models were measured with infrared thermography, as depicted in Fig. 2. It turned out that the surface temperatures are almost independent of the relative distribution of volume flow between the air inlets. Fig. 2 corresponds to a setting of equal volume flow rates through the air inlets. Due to the constant heat flux mode the temperatures are biased by the average cabin air temperature. Therefore only the temperature differences  $\Delta T_K$  with respect to the mean cabin air temperature are plotted. The passenger dummies reveal average surface temperatures of approximately  $\Delta T_K = 10$  K in the head region, which decrease on the clothes and the arms to approximately  $\Delta T_K = 5$  K. Since the legs of the passenger models are not heated, they exhibit no difference to the cabin air temperature. This explains the energy excess of a real passenger to our models.

The lateral light band models reveal surface temperature differences of  $\Delta T_K = 45$  K, while the light band models at the ceiling exhibit temperature differences of  $\Delta T_K = 55$  K due to the prevention of natural convection by the geometrical arrangement.

The velocity and temperature fields discussed in the following were measured in the cabin cross section between the third and fourth seat row.

## 3 Particle Image Velocimetry of Aircraft Cabin Air Flow

For determination of the fluid velocity in our cabin model Particle Image Velocimetry

(PIV) was used [9]: The flow in the cabin model was seeded with small tracer particles, which were illuminated by a light sheet of a laser pulse. An image of the illuminated particles was recorded by a CCD-camera. After a delay of the order of milliseconds, the particles were illuminated by a second laser pulse and a second picture of the particles was recorded. During the time delay the particles have moved according to the fluid velocity. The local displacement of the particles between the two pictures is thus a measure of the local fluid velocity, which can be determined precisely with local cross correlation algorithms. As a result, the velocity components of the fluid in the light sheet plane can be determined.

### 3.1 Experimental Set-Up

In order to measure the velocity fields of the flow in our aircraft cabin mock-up neutrally buoyant helium filled soap bubbles (HFSBs) with diameters between 0.2 and 0.3 mm have been injected into the flow. The bubbles were injected into the measurement plane directly at the air inlets where the momentum of the cabin flow is high and the disturbance due to the nozzle flow thus negligible. The bubbles were generated with orifice type nozzles [7][7] and a home-made bubble generator which was able to

operate three nozzles in parallel. As bubble fluid solution (BFS) a commercially available mixture of water, glycerin and soap was used. The generator and the nozzles are described in detail elsewhere [7].

While in PTV or PSV with continuous light sources HFSBs with diameters between 2 and 7 mm are used, PIV involving Nd:YAG lasers as light source, as described in the following, can be performed with much smaller particles. The benefits of using small HFSBs are

- less momentum input into the flow
- higher generation efficiency,
- higher sensitivity to small structures in the flow
- less consumption of BFS and thus less pollution of the model.

Consequently for PIV small HFSBs should be used preferably as long as the scattering efficiency is not the limiting factor for an actual measurement.

For illumination of the bubbles the nano-second laser pulses of a Nd:YAG double oscillator laser system (TwinsB, Quantel) with a pulse energy of 350 mJ/pulse were used. The laser light was shaped into a light sheet with a thickness between 3 and 5 cm in the observation area with a telescope and a cylindrical lens. A narrow viewport at the bottom of the mock-up allowed for coupling the laser light into the cabin from the basement, see Fig. 3. The flash lamps of the laser were operated at 10 Hz.

Two CCD cameras (Sensicam QE, PCO) were used in parallel in order to detect the particles. They were equipped with a Peltier-cooled CCD-chip with a resolution of 1376x1040 pixels. One camera was combined with a 21 mm lens (Distagon T\* 2.8/21, Carl Zeiss) and covered the large field of view (FOV 1), see Fig. 3, which amounted to 60 percent of the cabin cross section. The second camera was equipped with a 50 mm lens (Planar T\* 1.5/50) and thus able to resolve the flow in the region close to the lateral air inlet, where the incoming air jet is still narrow, with a higher resolution (FOV 2).

Since low frequency phenomena might occur in mixed convection in our mock-up, the PIV was extended over a period of 30 minutes. During this time, an image pair was recorded

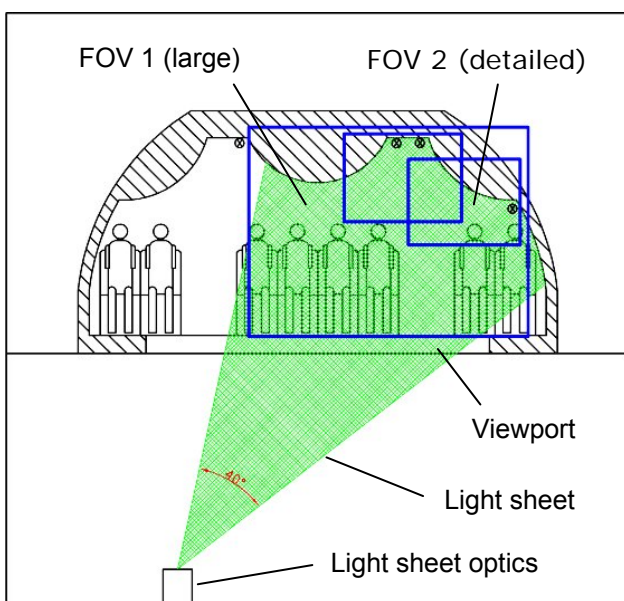


**Fig. 3:** Optical set up for PIV in the cabin mock-up on two floors.

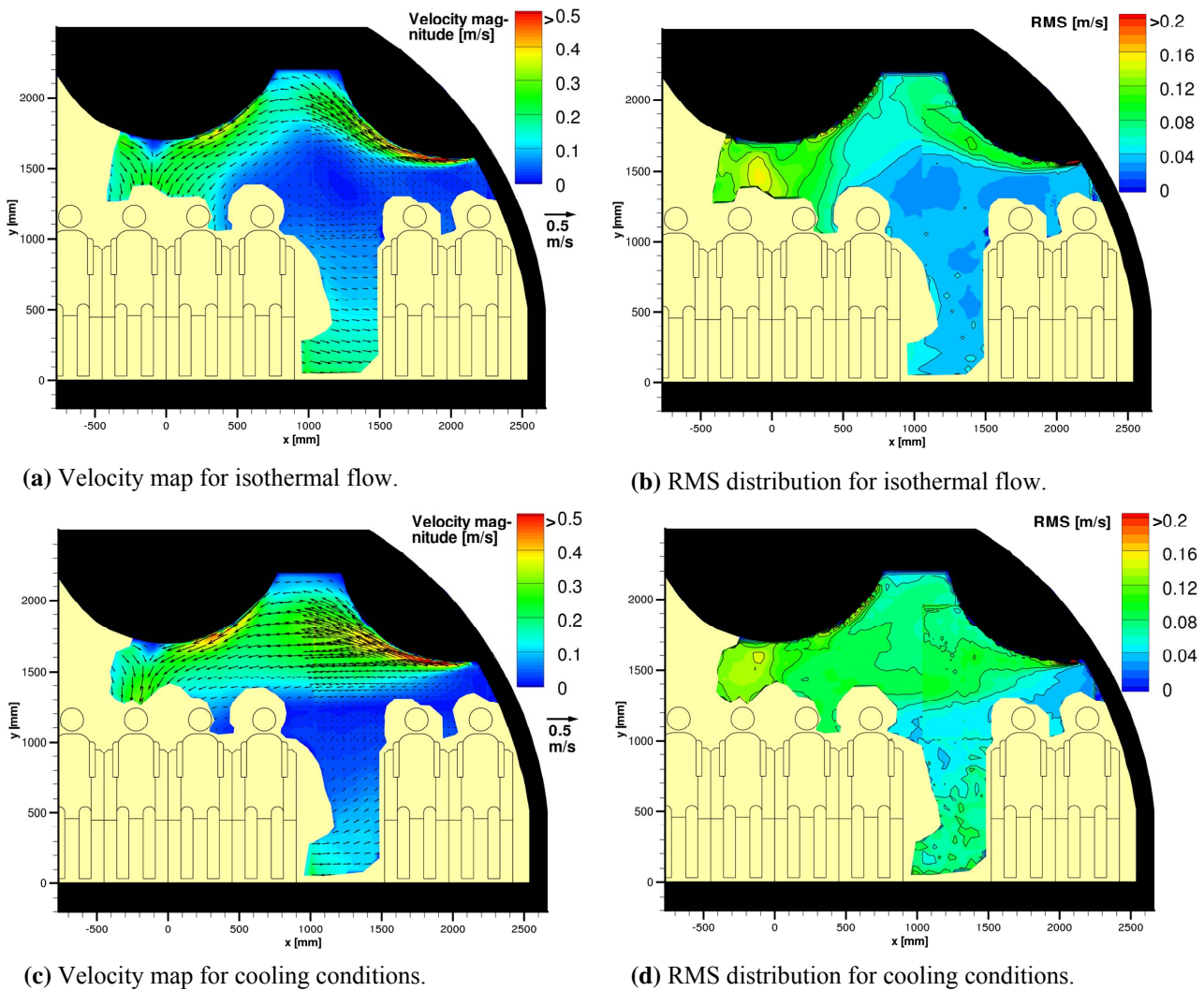


**Fig. 4.** Air flow in the A380 aircraft cabin mock-up studied with large-scale 2C-2D PIV under isothermal and cooling conditions. The left hand plots depict the average in-plane velocity as determined from 360 instantaneous velocity maps. For the large and small FOV only every 4th and 9th vector is plotted, respectively. The right hand plots show the corresponding RMS values. The central and lateral air inlets supplied 50% of the overall air flow each.

with both cameras every 5 seconds with subsequent pairs of laser pulses.

In order to determine the velocity fields a multiple pass interrogation algorithm was used for calculation of the correlation between the interrogation windows of subsequent images. The correlation maximum was determined with subpixel accuracy using WHITTAKER reconstruction. In order to further reduce noise, double correlation was applied. The interrogation window overlap was set to 50 % according to the NYQUIST theorem. Interrogation windows of 32x32 pixels were used for both FOVs leading to an interrogation window size of 72x72 mm<sup>2</sup> and 30x30 mm<sup>2</sup> for the large and detailed

FOV, respectively. The thickness of the light sheet is thus of the order of the interrogation window size as it is appropriate for highly 3D convective airflow.

### 3.2 Discussion of the Results

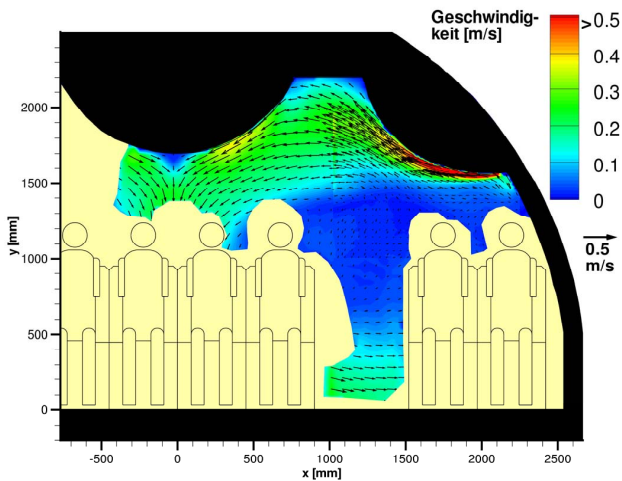
Fig. 4 depicts the velocity fields for equal mass flow distribution between the central and lateral air inlets, which supplied 50% of the overall air flow each. Results are given for both, isothermal and cooling conditions. The left hand plots depict the average in-plane velocity as determined from 360 instantaneous velocity maps. The right hand plots reveal the corresponding

RMS data of the deviations from the mean velocity in the 360 instantaneous velocity fields.

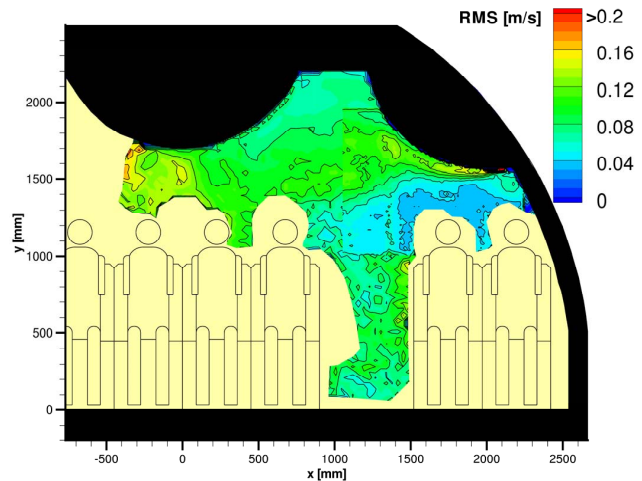
After entering the cabin, the incoming air jets directly attach to the overhead bin under isothermal conditions as well as in the cooling case.

Under isothermal conditions the lateral jet follows the overhead bin contour until it reaches the ceiling, where it separates and gets entrained by the jet from the air inlet at the ceiling. The combined jets follow the central overhead bin until they meet their counterpart from the other cabin side in the center of the cross section. A

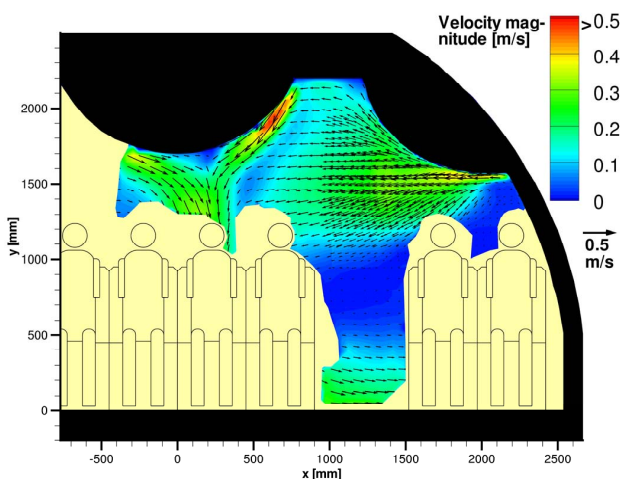
stagnation point develops and the jets from both cabin sides separate from the contour and move down to the floor. Here, a second stagnation point (not visible in the PIV measurement) causes division of the combined jets into two parts, which move to the air outlets on the right and left cabin wall. The maximal velocity in the passenger area is observed below the central overhead bin contour, and it amounts to 0.23 m/s. The RMS distribution (Fig. 4 (b)) reveals fluctuations in the jet region of approximately 0.1 m/s and much lower values of round about 0.03 m/s in almost the complete remain-



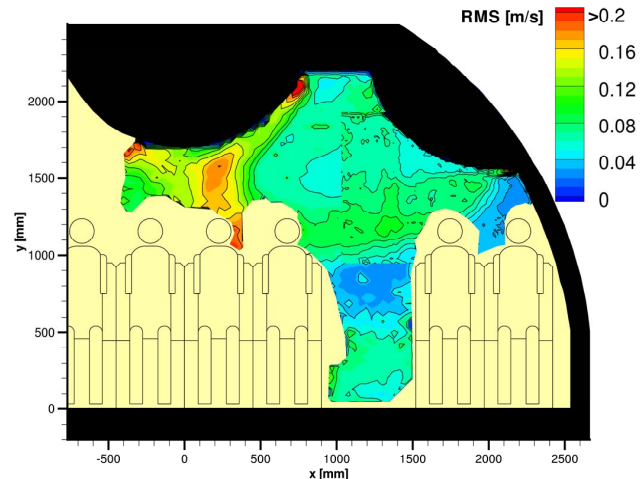
(a) Velocity field for 33 % volume flow from the ceiling, and 67 % from the lateral air inlets.



(b) RMS distribution for 33 % volume flow from the ceiling, and 67 % from the lateral air inlets.



(c) Velocity field for 67 % volume flow from the ceiling, and 33 % from the lateral air inlets.



(d) RMS distribution for 67 % volume flow from the ceiling, and 33 % from the lateral air inlets.

**Fig. 5.** Air flow in the A380 aircraft cabin mock-up studied with large-scale 2C-2D PIV under cooling conditions for two relative distributions of the volume flow rate. The left hand plots depict the average in-plane velocity as determined from 360 instantaneous velocity maps. For the large and small FOV only every 4th and 9th vector is plotted, respectively. The right hand plots show the corresponding RMS values.

ing area. Locally increased RMS values are observed at the separation points at the ceiling and at the central overhead bin, indicating instationary motion of the separation and stagnation points.

With the onset of thermal convection the flow in the mock-up changes significantly. Under cooling conditions the position of the stagnation point at the central overhead bin becomes strongly asymmetric with respect to the cabin geometry. The lateral air jet becomes much wider due to interaction with thermal convection from the passenger dummies. Substantial changes can be observed in the RMS distribution as well. The cooling case reveals a much more homogeneous distribution of the RMS values, which indicates a better mixing behavior with the onset of thermal convection. The increased values in the head region of the far right passenger dummy in the middle seat row indicate better accommodation of fresh air by the lateral air jet in this region, although the average velocity is close to zero. The maximal velocity in the passenger area occurs below the central overhead bin contour and rises to values of up to 0.29 m/s under cooling conditions, while the fluctuations decrease from 0.15 m/s to 0.13 m/s.

As the next step the relative mass flow between the ceiling and the lateral air inlets has been varied in order to investigate the influence of inertia forces on the flow field. Fig. 5 depicts the air flow in the A380 aircraft cabin mock-up as measured with large-scale PIV under cooling conditions for two relative distributions of the volume flow rate. In the first case, Fig. 5 (a) and (b), 67 % of the mass flow is injected through the lateral air inlets and only 33 % through the ceiling inlets. While the overall flow field does not change upon this parameter variation it can be seen clearly, that the separation point of the lateral air jet is shifted closer to the ceiling due to the increased momentum. The stagnation point below the central overhead bin is symmetrical in contrast to the equal distribution of volume flow rates in Fig. 4 (c). In the second case, Fig. 5 (c) and (d), 33 % of the mass flow is injected through the lateral air inlets and 67 % through the ceiling inlets. As a consequence of the reduced momentum of the lateral air jet the

separation point is shifted away from the ceiling as compared to the equal distribution of volume flow rates. Due to entrainment of surrounding air the ceiling air jet induces a force on the lateral jet which antagonizes the COANDA force. After a critical length the lateral air jet has lost too much momentum due to the action of the wall shear stress that it separates in order to get entrained by the ceiling air jet. Consequently the lateral air jets separate the sooner the lower their momentum, i.e. for a fixed outlet cross section the lower their relative mass flow. The stagnation point at the central overhead bin becomes strongly asymmetrical and the lateral air jet spreads over a large fraction of the cabin cross section due to additional dissipation of momentum due to interaction with thermal convection from the passenger dummies and the action of gravity.

The RMS maps (Fig. 4 (d), Fig. 5 (b), (d)) reveal that the distribution of velocity fluctuations is affected severely by the relative mass flow of the air inlets. The most inhomogeneous distribution was found for the case in Fig. 5 (c, d), where the air flow of the lateral air jet is minimal. In this case the maximal RMS values, which are as large as 0.18 m/s, are observed below the central overhead bin.

## 4 Measurement of Temperature Fields

### 4.1 Experimental Set-Up

As already stated, the passenger comfort in our aircraft cabin mock-up depends strongly upon the actual occurrence of premature jet separation. In order to judge the thermal comfort, however, the fluid temperature has to be determined in addition. Therefore the average air temperature was measured with a thermocouple rake. The rake consisted of 26 type-K thermocouples which were arranged in a horizontal line. It was scanned vertically through the mock-up, while at each position the temperatures were averaged over a period of 10 minutes. The resulting temperature distributions are depicted in Fig. 6 together with the velocity maps, which have already been shown in Fig. 5

and Fig. 4. Since the temperature of the room, which surrounds the cabin model, could not be controlled during measurement, the average temperature in the mock-up slowly changed in time with 0.25 K per hour. For the PIV measurements, taking 30 minutes to perform, this can be neglected. The temperatures, however, measured by scanning the mock-up had to be corrected with the mean temperature of the air in the mock-up for each measurement position, which was controlled with another permanently installed measurement system. In order to compensate for the slightly increasing average cabin temperature during the measurement, the locally measured temperature deviations from the inflow temperature ( $T - T_{in}$ ) were normalized with the global temperature difference  $\Delta T$  between incoming air and the air in the mock-up at the moment of the actual measurement and the average global temperature difference  $\langle \Delta T \rangle$ . The corrected local temperature deviations  $\Delta T_{loc}$  were determined via

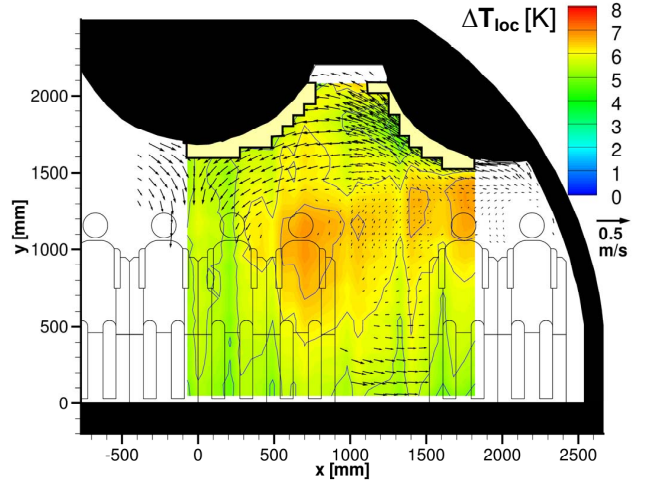
$$\Delta T_{loc} = (T - T_{in}) \frac{\langle \Delta T \rangle}{\Delta T} \quad (1)$$

This correction reflects the fact that the fraction  $(T - T_{in}) / \Delta T$  is proportional to the local air exchange rate which, in turn, is given by the velocity field. Our temperature correction is thus valid as long as the temperature drift is small enough in order that it does not severely affect the velocity field, which is the case in our measurements.

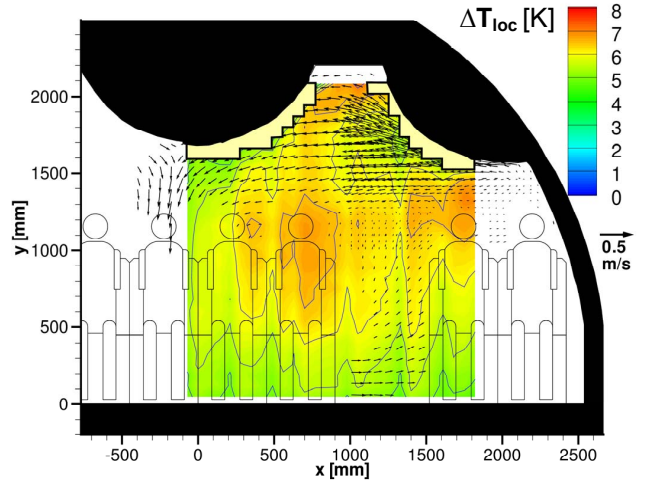
#### 4.2 Discussion of the Results

In Fig. 6 the average temperature and velocity fields as measured in the A380 aircraft cabin mock-up under cooling conditions are given for three different relative distributions of volume flow between the air inlets. The contours depict the  $\Delta T_{loc}$ , while the vector fields show the velocity maps from Fig. 4 and Fig. 5.

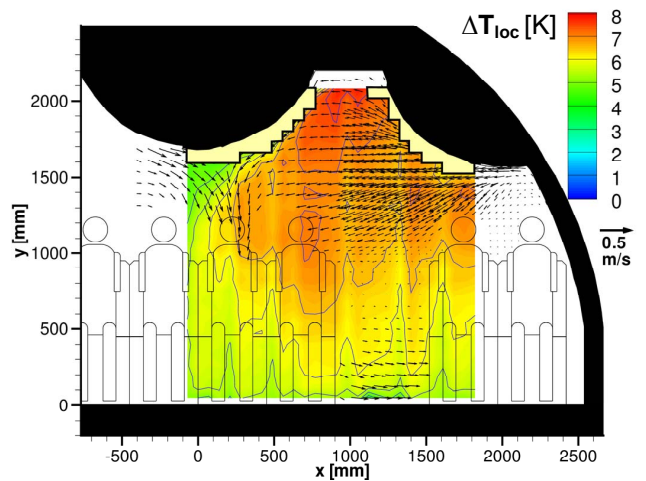
Clearly the pathways of the air jets can be detected by a reduced temperature as compared to the mean cabin temperature.



(a) 33 % volume flow from the ceiling, and 67 % from the lateral air inlets.



(b) 50 % volume flow from the ceiling, and 50 % from the lateral air inlets.



(c) 67 % volume flow from the ceiling, and 33 % from the lateral air inlets.

**Fig. 6.** Average temperature and velocity fields as measured in the A380 aircraft cabin mock-up under cooling conditions. The contours depict the local temperature difference  $\Delta T_{loc}$ , see text, while the vector fields show the velocity maps from Fig. 4 and Fig. 5.

With reduction of the volume flow rate from 33 % over 50 % to 67 % the  $\Delta T_{loc}$  of the separating central ceiling jets decreases from 5.4 over 5.0 to 4.6 K, respectively. The reason is that with increasing relative flow rate the cold air from the ceiling inlets has to travel a shorter downstream distance and has thus fewer occasions to mix up with the cabin air before separation. The local  $\Delta T$  in the foot region on the other hand is almost unaffected by the relative distribution of mass flow and amounts to values around 5.3 K.

With reduction of the volume flow rate from 33 % over 50 % to 67 % the  $\Delta T_{loc}$  at the ceiling on the other hand increases from 6.4 over 7.0 to 7.8 K, respectively, until in the last case a temperature stratification of 2.5 K from the floor to the ceiling develops. The reason for this behavior is that with decreasing mass flow of the lateral air inlets less cool air is brought to the upper region in the cabin and thus less heat is removed. For the head region of the passenger dummies this leads to a significant increase in  $\Delta T_{loc}$  and to a more inhomogeneous temperature distribution in the mock-up.

### Summary / Conclusions

Mixed convection has been investigated with large scale Particle Image Velocimetry, infrared thermography, and temperature field measurements in a full scale double aisle aircraft cabin mock-up. Detailed control of the thermal boundary conditions and adaptation of the geometrical boundary conditions to the needs of both Computational Fluid Dynamics as well as optical field measurement techniques qualifies our mock-up as a testing configuration for CFD-simulations and validation measurements.

Independently the influence of buoyancy and jet-jet interaction has been studied by systematic variation of the relative distribution of volume flow between the air inlets and by switching from isothermal to cooling conditions. The resulting flow fields have been determined quantitatively with high accuracy by application of helium filled soap bubbles as

tracer particles for PIV. Features of the flow like separation lines, stagnation points, jet profiles and their fluctuations are important measures for the rating of numerical simulations. Their dependence on the operational parameters gives insight into the mechanisms, which determine the local climate in an aircraft cabin. Finally the thermal characteristics of the flow fields have been revealed by measurement of the field temperature distributions using thermocouple rakes.

### References

- [1] Mo H, Hosni MH and Jones BW. Application of Particle Image Velocimetry for the Measurement of the Airflow Characteristics in an Aircraft. *ASHRAE Transactions*, Vol. 109, pp 101-110, 2003.
- [2] Müller RHG, Scherer T, Rötger T, Schaumann O and Markwart M. Large Body Aircraft Cabin A/C Flow Measurement by Helium Bubble Tracking. *Journal of Flow Visualization and Image Processing*, Vol. 4, pp 295-306, 1997.
- [3] Müller RHG and Flögel H. Investigation of Large Scale Low Speed Condition Flow using PIV. *Proc. 9th Int. Symposium on Flow Visualization*, Edinburgh, 218, pp 1 - 12, 2000.
- [4] Sun Y, Zhang Y, Wang A, Topmiller JL and Bennett JS. Experimental Characterization of Airflows in Aircraft Cabins, Part I: Experimental System and Measurement Procedure. *ASHRAE Transactions*, Vol. 111, pp 45-52, 2005.
- [5] Zhang Y, Sun Y, Wang A, Topmiller JL and Bennett JS. Experimental Characterization of Airflows in Aircraft Cabins, Part II: Results and Research Recommendations. *ASHRAE Transactions*, Vol. 111, pp 53-59, 2005.
- [6] Bosbach J, Penneçot J, Wagner C, Raffel M, Lerche T and Repp S. Experimental and numerical simulations of turbulent ventilation in aircraft cabins. *Energy*, Vol. 31, pp 694-705, 2006.
- [7] Bosbach J, Kühn M, Wagner C, Raffel M, Resagk C, du Puits R, Thess A. Large Scale Particle Image Velocimetry of Natural and Mixed Convection. Proceedings of the 13<sup>th</sup> International Symposium on Applications of Laser Techniques to Fluid Mechanics, Paper No. 1182, Lisbon, Portugal, 2006.
- [8] Okuno Y, Fukuda T, Miwate Y and Kobayashi T. Development of Three Dimensional Air Flow Measuring Method Using Soap Bubbles. *JSAE Review*, Vol 14, pp 50-55, 1993.
- [9] Raffel M, Willert CE and Kompenhans J. *Particle Image Velocimetry – A practical Guide*. 1<sup>st</sup> edition, Springer-Verlag, Berlin, 1997.